Plasmonics (2011) 6:619–624
DOI 10.1007/s11468-011-9243-2

Nanoscale Surface Plasmon All-Optical Diode Based on Plasmonic Slot Waveguides

Xiaoyong Hu · Yingbo Zhang · Xinan Xu · Qihuang Gong

Received: 14 March 2011 / Accepted: 23 May 2011 / Published online: 31 May 2011

Abstract A nanoscale surface plasmon all-optical diode is proposed based on a plasmonic slot waveguide having an asymmetric plasmonic grating in the center. The asymmetric configuration of the plasmonic grating and the unique dispersion relations of the plasmonic slot waveguide ensure the nonreciprocal transmission properties. High transmittance contrast ratio of 1,150 is achieved theoretically. The performance of the surface plasmon all-optical diode does not have any high power requirement. This may open a new way for the study of integrated photonic devices based on surface plasmons.

Keywords Surface plasmon · All-optical diode · Plasmonic slot waveguide

Introduction

Nanoscale all-optical diode is one of the essential components of optical computing, optical interconnection systems, and integrated photonic circuits. Analogous to its electronic counterparts, nanoscale all-optical diode has nonreciprocal transmission properties, i.e., transmitting light in one direction and blocking it in the reverse direction. There are two key characteristics for nanoscale all-optical diodes: low operating threshold power and high transmission contrast, which is defined as the ratio of maximum transmission in one direction to the corresponding transmission in the reverse direction. Various schemes have been proposed to demonstrate nanoscale all-optical diodes, including using nonlinear photonic crystal and photonic bandgap microcavities [1–5], chiral photonic crystals with an anisotropic defect layer [6], left-handed periodic structures with a Kerr nonlinear defect layer [7], low-symmetry magnetic photonic crystals [8], periodically poled lithium niobate waveguides [9], and photonic crystal fibers [10, 11]. However, owing to the relatively small nonlinear optical susceptibility and magneto-optical coefficient of conventional materials, the operating threshold intensity is very high, often in several gigawatts per cubic centimeter order [9–11]. Moreover, the achieved transmittance contrast is very low, usually less than 90 [9–14]. Recently, Hwang and Song pointed out that it is possible to realize low-power all-optical diodes by combining the photonic bandgap effect and the unique interface properties of asymmetric liquid-crystal photonic bandgap heterostructure, without adopting any optical nonlinearity [15, 16]. Subsequently, Cakmakyapan et al. reported a low-power all-optical diode in an asymmetric metallic grating heterostructure with a subwavelength slit [17]. Our group also realized a low-power all-optical diode based on tunable surface plasmon polaritons (SPPs) in a silver grating coated with nonlinear optical material [18]. However, the propagation direction of the signal light is perpendicular to the metal film [17, 18]. This makes the all-optical diode unsuitable for the practical integration applications.

The aim of this letter is to study how to realize a low-power and high-contrast nanoscale surface plasmon (SP) all-optical diode suitable for the practical on-chip integration applications. For this purpose, we adopted a plasmonic slot waveguide consisting of a silicon waveguide sandwiched between two silver films, as previously used by Dionne et al.

X. Hu (✉) · Y. Zhang · X. Xu · Q. Gong (✉)
State Key Laboratory for Mesoscopic Physics
and Department of Physics, Peking University,
Beijing 100871, People's Republic of China
e-mail: xiaoyonghu@pku.edu.cn

Q. Gong
e-mail: qhgong@pku.edu.cn

[19]. The plasmonic slot waveguide provides the transverse magnetic (TM) polarized SP modes, which are strongly confined in the interface of the dielectric waveguide and metal films [19]. The electric field distribution of TM_0 SP modes is symmetric with respect to the silicon waveguide, while that of the TM_1 SP modes is asymmetric with respect to the silicon waveguide [19]. The TM SP modes propagate in the direction parallel to the silver films, which is suitable for the on-chip integration applications. To achieve the nonreciprocal transmission properties, an asymmetric plasmonic grating, having a grating formed in the upside of the silicon film, and a grating with a scattering block in its right side, formed in the downside of the silicon film, was placed in the center of the plasmonic slot waveguide. Barnes et al. and Balci et al. have pointed out that a stop band for the SP modes will be formed when the grating period is nearly half of the SP wavelength [20, 21]. The structural parameters of the plasmonic grating were carefully designed, so that the stop band of the TM_0 SP modes overlaps a part with that of the TM_1 SP modes. A symmetric SP mode, whose resonant frequency dropping in the TM_0 stop band, but within the TM_1 pass band, was used as the signal light. A part of the energy of signal light can be transferred into the asymmetric SP mode due to the strong scattering effect of the scattering block, which has been confirmed by Zayats et al. [22]. Therefore, when the signal light is launched from the right side, it is firstly transferred into the TM_1 mode by the scattering block and subsequently propagates through the grating region. The signal can propagate through the plasmonic slot waveguide in the direction from right to left side. When the signal light is launched from the left side, it will be reflected completely by the plasmonic grating because its frequency was located in the TM_0 stop band. Therefore, a nanoscale SP all-optical diode can be achieved without any high power requirement.

Simulation Model

The schematic structure of the plasmonic slot waveguide, consisting of a silicon waveguide sandwiched between two silver films, is shown in Fig. 1, as previously used by Dionne et al. [19]. An asymmetric plasmonic grating, having a grating formed in the upside of the silicon film and a grating with a scattering block in its right side formed in the downside silicon film, is placed in the center of the plasmonic slot waveguide. The plasmonic slot waveguide is finite in the *z* direction, while infinite in *x* and *y* directions. In order to benefit the practical experiment measurements, the thickness of input and output part of the silicon was enlarged. The length of the grooves of the plasmonic grating is infinite in the *y* direction. h_1, h_2, h_3, h_4, and h_5 represent the depth of the grooves, depth of the scattering block B, the thickness of the silicon waveguide in the center, the thickness of the silver films, and the thickness of the input/output side of silicon waveguide, respectively. *a* and *l* were the lattice constant and the width of the grooves, respectively. The finite-difference time-domain (FDTD) method (using a commercial software RemCom XFDTD, version 6.4.18.2) was used to study the transmission properties [23]. In our calculation, h_1, h_2, h_3, h_4, and h_5 were set at 100, 225, 600, 1,000, and 1,200 nm, respectively. *a* and *l* were set at 500 and 250 nm, respectively. The dielectric constant of silicon was 11.56. The complex permittivity of silver were obtained from Johnson and Christy's experimental data [24] and fitted with the Drude model to conduct the calculations of the dispersion relation and the transmission properties of the plasmonic slot waveguide, as previously done by Kim et al. [25]. A 1638-nm symmetric SP mode, belonging to a TM_0 mode, was used as the signal light. The propagation direction of the signal light is perpendicular to the grooves, i.e., along the *x* direction.

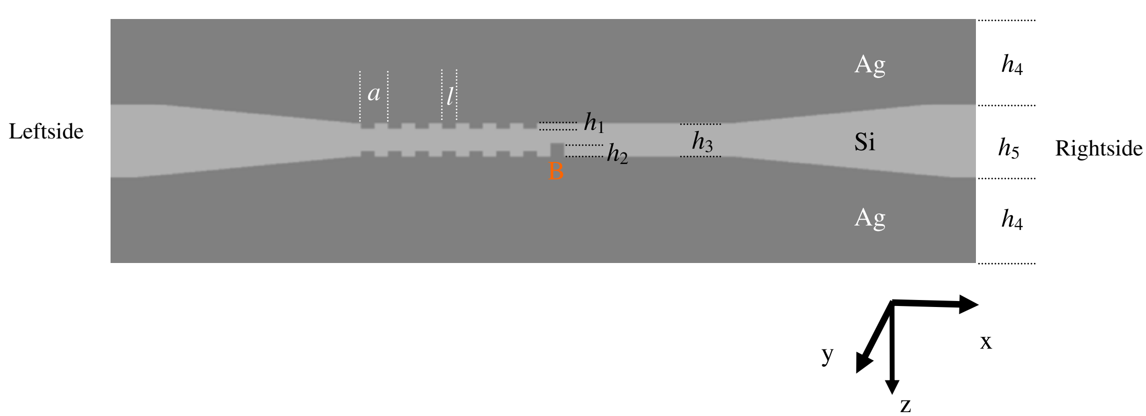

Fig. 1 Schematic structure of the plasmonic slot waveguide

Dispersion Relation Properties

We calculated the dispersion relations of the plasmonic slot waveguide in the low-frequency range with and without the plasmonic grating, and the results are shown in Fig. 2. The scattering block B was not included in the calculation of the dispersion relation. It is very clear that the plasmonic slot waveguide can provide TM-polarized SP modes. There were several continuous TM pass bands for the plasmonic slot waveguide without the plasmonic grating. We only showed three low-order TM bands, i.e., TM_0, TM_1, and TM_2 band in Fig. 2a. When the plasmonic grating was placed in the center of the plasmonic slot structure, stop bands appeared in the dispersion relation curves, as shown in Fig. 2b. The reason lies in that when the period of the plasmonic grating is half the wavelength of the SP modes, the strong Bragg scattering will lead to the formation of stop bands in the dispersion diagrams [20]. The stop band covered the frequency range from 0.5156 to 0.7058 $2\pi c/a$ for TM_0 modes and from 0.6522 to 1.0328 $2\pi c/a$ for TM_1 modes, respectively. So, the stop band of TM_0 modes overlaps with that of TM_1 modes in the frequency range from 0.6522 to 0.7058 $2\pi c/a$. As a result, a symmetric SP mode with a resonant frequency of 0.6106 $2\pi c/a$, corresponding to the wavelength of 1,638 nm, drops in the stop band of TM_0 modes but within the pass band of TM_1 modes, as shown in Fig. 2b.

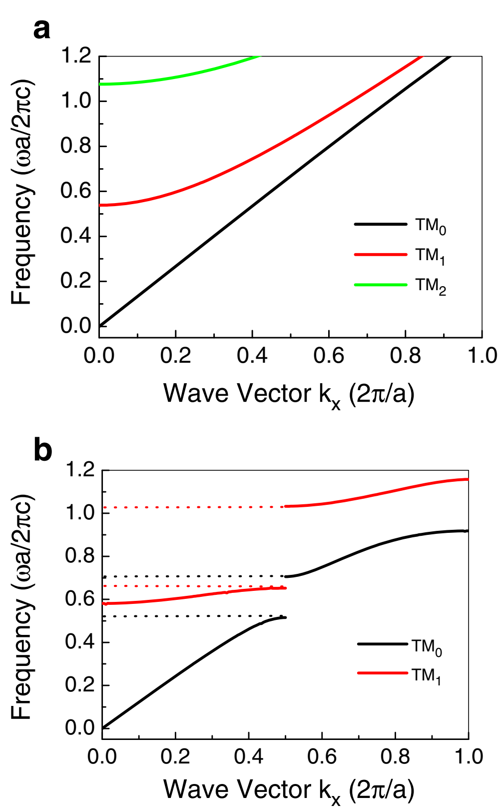

Fig. 2 Dispersion relations of the plasmonic slot waveguide for the low-frequency range. **a** Without the grating structure. **b** With the grating structure but without the scattering block B

All-Optical Diode Performances

To study the all-optical diode functions, we calculated the electric filed distribution of the signal light, the 1,638-nm symmetric SP (belonging to TM_0 mode), through the plasmonic slot waveguide by use of the FDTD method, and the results are shown in Fig. 3. The 1,638-nm symmetric SP drops in the stop band of TM_0 modes, but within the pass band of TM_1 modes, as shown in Fig. 2b. For the left side incidence case, the 1,638-nm symmetric SP entered the plasmonic grating directly. So, the 1,638-nm symmetric SP was reflected completely by the plasmonic grating because of the strong stop band effect of TM_0 modes. Therefore, the signal light could not propagate through the plasmonic slot waveguide in the direction from the left side to the right side. The case changed when the signal light was incident from the opposite direction. For the right side incidence case, a part of the energy of the 1,638-nm symmetric SP was firstly transferred into an asymmetric mode by the scattering block B and subsequently entered the plasmonic grating. The 1,638-nm asymmetric SPP mode is situated in the pass band of the TM_1 modes. So, the signal light could propagate through the plasmonic grating. Therefore, the signal light could propagate through the plasmonic slot waveguide in the direction from the right side to the left side. An all-optical diode is realized based on the plasmonic slot waveguide without any high power requirement.

To further confirm the all-optical diode function of the plasmonic slot waveguide, we calculated the transmittance spectra of the plasmonic slot waveguide for the 1,638-nm symmetric SP as a function of the number of the grating period, and the calculated results are shown in Fig. 4. When the grating period number was 6, the transmittance of the 1,638-nm symmetric SP was 23% for the right side incidence case and 0.02% for the left side incidence case, respectively. Therefore, high transmission contrast of 1,150 was realized, which is about two orders of magnitude larger than that of the previously reported results [1–14]. High transmission contrast is an indispensable and essential index for all-optical diode. In practical applications, the all-optical diode with a low transmission contrast will bring about a serious signal crosstalk. With the increase of the grating period number, the transmittance of the 1,638-nm signal light decreased remarkably for the right side incidence case. When the period number of the plasmonic grating increased from 6 to 20, the transmittance of the

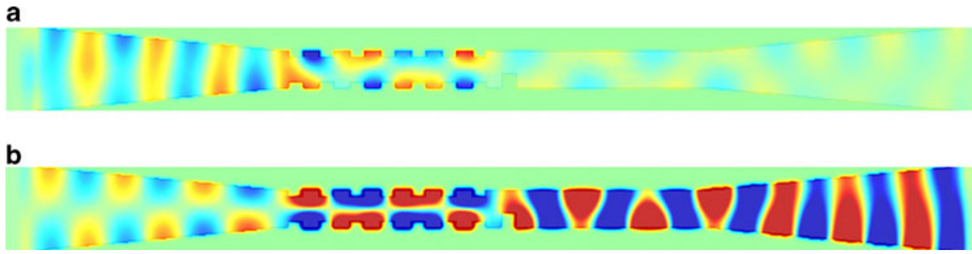

Fig. 3 Electric field distribution of the 1,638-nm TM_0 mode. **a** For the left side incidence case. **b** For the right side incidence case

signal light decreased from 23% to 3%. The reason may lie in the strong scattering loss and the intrinsic loss of silver originating from the large imaginary part of the permittivity [26]. However, more than 10% transmittance can still be achieved when the period number of the plasmonic grating is less than 10. For the left side incidence case, the transmittance of the 1,638-nm signal light also decreased. But, the magnitude of the decrease was not very obvious because the signal light can only enter few lattices due to the strong stop band effect. So, the increase of the period number of the plasmonic grating has a small influence on the transmittance of the left side incidence case.

The above results are carried out by the calculation of the perfect plasmonic grating structure. But, in practice, when a plasmonic grating is fabricated, the structural disorders cannot be removed, which can alter the photonic band structure of the plasmonic grating. To study the influences of structural disorders of the plasmonic grating on the function of the all-optical diode, we calculated the transmittance changes of the plasmonic slot waveguide for the 1,638-nm symmetric SP with various degrees of disorders caused by the perturbations in the depth of the grooves, and the calculated results are shown in Fig. 5a. The period number of the plasmonic grating was set at 6. The disorder degree δ is used to describe the deviation in the depth of the grating grooves. The depth of the grating grooves is randomly distributed in the interval from $h_1(1-\delta)$ to $h_1(1+\delta)$. So, the depth of the grating grooves can be calculated by $h_1(1+\Delta\delta)$, where Δ is a random number in the range of (−1,1). With the increase of the disorder degree of grating groove depth, the transmittance of the 1,638-nm signal light decreased remarkably for the right side incidence case. When the disorder degree increased from zero to 30%, the transmittance of the signal light decreased from 23% to less than 5%. The perfect photonic bandgap structure of TM modes will be destroyed seriously with the increase of the disorder degree. For the right side incidence case, the 1,638-nm signal light was transferred into the asymmetric TM_1 mode by the scattering

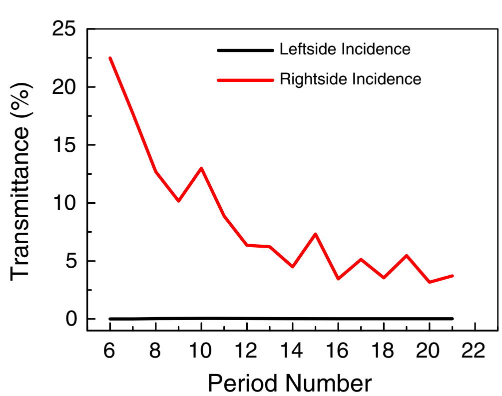

Fig. 4 Transmittance changes of the plasmonic slot waveguide for the 1,638-nm TM_0 mode with different period number of the plasmonic grating

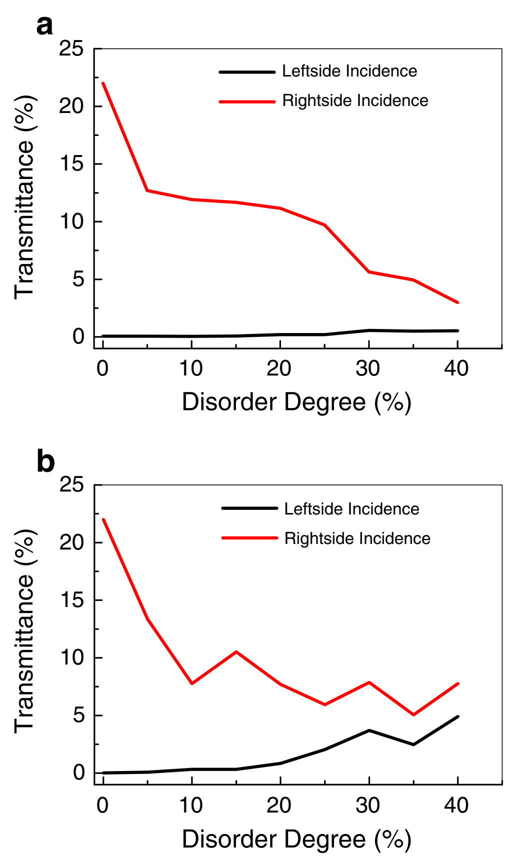

Fig. 5 Transmittance changes of the plasmonic slot waveguide for the 1,638-nm TM_0 mode with various structural disorders of the plasmonic grating. **a** For the depth disorder of the grating grooves. **b** For the width disorder of the grating grooves

block B, which makes the signal light in the pass band of TM_1 modes. McGurn et al. pointed out that structural disorders could result in the exponential attenuation of light in the pass band, which makes the transmittance of the pass band decrease [27]. This makes the transmittance of the signal light decrease. However, when less than 10% disorder degree was introduced, more than 13% transmittance can still be reached for the right side incidence case. For the left side incidence case, the signal light was located in the stop band of TM_0 modes. With the increase of the disorder degree of the grating groove depth, the transmittance of the 1,638-nm signal light increased gradually for the left side incidence case. When the disorder degree increased from zero to 30%, the transmittance of the signal light increased from 0.02% to less than 0.65%. Frigerio et al. pointed out that structural disorders could lead to the presence of the band-tail states and localized defect states in the stop band, which strengthen the transmittance of the stop band [28]. However, when less than 10% disorder degree was introduced, the transmittance was less than 0.021% for the left side incidence case. Therefore, a high transmission contrast of over 600 can still be reached. This indicates that a certain range of the degrees of the depth disorder of the plasmonic grating grooves is acceptable to the all-optical diode. Figure 5b shows the transmittance changes of the plasmonic slot waveguide for the 1,638-nm symmetric SPP wave with various degrees of disorders caused by the perturbations in the width of the grating grooves. The width of the plasmonic grating grooves l can be calculated by $l(1+\Delta\delta)$, where Δ is a random number in the range of $(-1,1)$, δ is the disorder degree. The maximum disorder degree δ makes two neighboring grooves connect with each other. Similarly, with the increase of disorder degrees, the transmittance of the right side incidence decreased and the transmittance of the left side incidence increased. When the disorder degree of less than 5% is introduced, a high transmittance of over 15% can be obtained for the right side incidence case, and a low transmittance of 0.022 can be reached for the left side incidence case. A high transmission contrast of 680 can still be achieved with a disorder degree of less than 5%. Therefore, when less than 5% structural disorder degree is introduced, the plasmonic slot waveguide can maintain the perfect functions of the all-optical diode. Our calculations mean that the all-optical diode can be achieved even if the plasmonic slot waveguide possesses a certain range of disorder degrees in the depth or width of the plasmonic grating grooves.

High-quality silver and silicon films can be fabricated very conveniently by a variety of thin-film growth techniques, such as the molecular-beam epitaxy method, the chemical vapor deposition method, and the magnetron sputtering method [29, 30]. The asymmetric plasmonic grating can be fabricated by use of the microfabrication techniques, such as the focused ion-beam etching method, the electron-beam lithography method, and so on [31]. Therefore, the sample of the plasmonic slot waveguide can be obtained easily in practice. The total size of the plasmonic slot waveguide is only in several microns order. The nanoscale SP all-optical diode does not have any high power requirement. Compared with previously reported all-optical diodes based on the nonlinear Kerr effect and the magneto-optic effect [9–14], the nanoscale SP all-optical diode possesses an ultralow-power and ultrahigh transmission contrast of the order of 10^3 simultaneously. Moreover, the propagation direction of the signal light is along the metal films. This makes the nanoscale SP all-optical diode much suitable for the practical integration applications. So, the applicability of the nanoscale SP all-optical diode is much better than that of the low-power all-optical diode based on metallic grating heterostructure [17, 18].

Conclusion

In conclusion, a nanoscale low-power SP all-optical diode was realized theoretically based on a plasmonic slot waveguide. A high transmission contrast of 1,150 was achieved. These results may be useful references for the study of integrated photonic devices. The beneficial effects of the nanoscale SP all-optical diode lie in that the nanoscale all-optical diode is not only an indispensable and essential component part of integrated photonic devices, including all-optical logic gate, all-optical memory, and all-optical adder unit, but can also be used to eliminate the signal crosstalk and help to reduce the device size effectively.

Acknowledgments This work was supported by the National Natural Science Foundation of China under grants 61077027, 10874010, 10821062, 90921008, and 10434020 and the National Basic Research Program of China under grant 2007CB307001.

References

1. Scalora M, Dowling JP, Bowden CM, Bloemer MJ (1994) The photonic band edge optical diode. J Appl Phys 76:2023–2026
2. Tocci MD, Bloemer MJ, Scalora M, Dowling JP, Bowden CM (1995) Thin-film nonlinear optical diode. Appl Phys Lett 66:2324–2326
3. Lin XS, Yan JH, Wu LJ, Lan S (2008) High transmission contrast for single resonator based all-optical diodes with pump-assisting. Opt Express 16:20949–20954
4. Zhou H, Zhou KF, Hu W, Guo Q, Lan S, Lin XS, Gopal AV (2006) All-optical diodes based on photonic crystal molecules consisting of nonlinear defect pairs. J Appl Phys 99:123111

5. Mingaleev SF, Kivshar YS (2002) Nonlinear transmission and light localization in photonic-crystal waveguides. J Opt Soc Am B 19:2241–2249
6. Gevorgyan AH, Harutyunyan MZ (2007) Chiral photonic crystals with an anisotropic defect layer. Phys Rev E 76:031701
7. Feise MW, Shadrivov IV, Kivshar YS (2005) Bistable diode action in left-handed periodic structures. Phys Rev E 71:037602
8. Khanikaev AB, Steel MJ (2009) Low-symmetry magnetic photonic crystals for nonreciprocal and unidirectional devices. Opt Express 17:5265–5272
9. Gallo K, Assanto G, Parameswaran KR, Fejer MM (2001) All-optical diode in a periodically poled lithium niobate waveguide. Appl Phys Lett 79:314–316
10. Konorov SO, Biryukov DAS, Bugar I, Beloglazov MJ, Skibina NB, Chorvatjr D, Chorvat D, Scalora M, Zheltikov AM (2004) Experimental demonstration of a photonic-crystal-fiber optical diode. Appl Phys B: Lasers Opt 34:1417–1420
11. Biryukov DAS, Fedotov AB, Konorov SO, Mitrokhin VP, Scalora M, Zheltikov AM (2004) Photonic crystal fiber optical diode. Laser Phys 14:764–766
12. Philip R, Anija M, Yelleswarapu CS, Rao DVGLN (2007) Passive all-optical diode using asymmetric nonlinear absorption. Appl Phys Lett 91:141118
13. Lin XS, Wu WQ, Zhou H, Zhou KF (2006) Enhancement of unidirectional transmission through the coupling of nonlinear photonic crystal defects. Opt Express 14:2429–2439
14. Zhao NS, Zhou H, Guo Q, Hu W, Yang XB, Lan S (2006) Design of highly efficient optical diodes based on the dynamics of nonlinear photonic crystal molecules. J Opt Soc Am B 23:2434–2240
15. Hwang J, Song MH, Park B, Nishimura S, Toyooka T, Wu JW, Takanishi Y, Ishikawa K, Takezoe H (2005) Electro-tunable optical diode based on photonic bandgap liquid-crystal heterojunctions. Nature Mater 4:383–387
16. Song MH, Park B, Takanishi Y, Ishikawa K, Nishimura S, Toyooka T, Takezoe H (2006) Simple electro-tunable optical diode using photonic and anisotropic liquid crystal films. Thin Solid Films 509:49–52
17. Cakmakyapan S, Caglayan H, Serebryannikov AE, Ozbay E (2011) Experimental validation of strong directional selectivity in nonsymmetric metallic gratings with a subwavelength slit. Appl Phys Lett 98:051103
18. Hu XY, Xin C, Li ZQ, Gong QH (2010) Ultrahigh-contrast all-optical diodes based on tunable surface plasmon polaritons. New J Phys 12:1023029
19. Dionne JA, Sweatlock LA, Atwater HA, Polman A (2006) Plasmon slot waveguides: towards chip-scale propagation with subwavelength-scale localization. Phys Rev B 73:035407
20. Barnes WL, Preist TW, Kitson SC, Sambles JR (1996) Physical origin of photonic energy gaps in the propagation of surface plasmons on gratings. Phys Rev B 54:6227–6244
21. Balci S, Kocabas A, Kocabas C, Aydinli A (2010) Slowing surface plasmon polaritons on plasmonic coupled cavities by tuning grating grooves. Appl Phys Lett 97:131103
22. Zayats AV, Smolyaninov II, Maradudin AA (2005) Nano-optics of surface plasmon polaritons. Phys Report 408:131–314
23. Ding CY, Hu XY, Jiang P, Gong QH (2008) Tunable surface plasmon polariton microcavity. Phys Lett A 372:4536–4538
24. Johnson PB, Christy RW (1972) Optical constant of the noble metals. Phys Rev B 6:4370–4379
25. Kim MK, Lee SH, Choi M, Ahn BH, Park N, Lee YH, Min B (2010) Low-loss surface-plasmonic nanobeam cavities. Opt Express 18:11089–11096
26. Kurokwaw Y, Miyazaki HT (2007) Metal-insulator-metal plasmon nanocavities: analysis of optical properties. Phys Rev B 75:035411
27. McGurn AB, Christensen KT, Mueller FM, Maradudin AA (1993) Anderson localization in one-dimensional randomly disordered optical system that are periodic on average. Phys Rev B 47:13120–13125
28. Frigerio JM, Rivory J, Sheng P (1993) Photonic bandtail in 1D randomly-perturbed periodic system. Opt Commun 98:231–235
29. Martinez A, Blasco J, Sanchis P, Galan JV, Ruperez JG, Jordana E, Gautier P, Lebour Y, Hernandez S, Guider R, Daldosso N, Garrido B, Fedeli JM, Pavesi L, Marti J (2010) Ultrafast all-optical switching in a silicon-nanocrystal-based silicon slot waveguide at telecom wavelengths. Nano Lett 10:1506–1511
30. Chang YT, Wu YT, Lee JH, Chen HH, Hsueh CY, Huang HF, Jiang YW, Chang PE, Lee SC (2009) Emission properties of Ag/dielectric/Ag plasmonic thermal emitter with different lattice type, hole shape, and dielectric material. Appl Phys Lett 95:213102
31. Briggs RM, Grandidier J, Burgos SP, Feigenbaum E, Atwater HA (2010) Efficient coupling between dielectric-loaded plasmonic and silicon photonic waveguides. Nano Lett 10:4851–4857